Evolution of paleo sea-surface conditions over the last 600 years in the Mackenzie Trough, Beaufort Sea (Canada)

Thomas Richerol [a],[*], André Rochon [a], Steve Blasco [b], Dave B. Scott [c], Trecia M. Schell [c], Robbie J. Bennett [b]

[a] UQAR–ISMER 310 Allée des Ursulines, Rimouski, QC, G5L 3A1 Canada
[b] Natural Resources Canada, Marine Environmental Geoscience, Bedford Institute of Oceanography, 1 Challenger Drive, Dartmouth, Nova Scotia, B2Y 4A2 Canada
[c] Centre for Environmental and Marine Geology, Dalhousie University, Halifax, Nova Scotia, B3H 3J5 Canada

ARTICLE INFO

ABSTRACT

In order to document long-term climate trends and predict future climate change for the Arctic, we need to look at the geological record to establish the link between historical and pre-industrial sea-surface parameters. Dinoflagellate cysts (dinocysts) are used as proxy indicators of sea-surface parameters (temperature, salinity, sea-ice cover, primary productivity) jointly with transfer functions and a modern dinocyst reference database, to reconstruct the evolution of sea-surface conditions at decadal and multi-decadal timescales.

Here we present the fossil dinocyst assemblages established from three sediment cores collected along an inshore–offshore transect in the Mackenzie Trough during the 2004 CASES (Canadian Arctic Shelf Exchange Study) cruise. The chronology of each core was determined using ^{210}Pb activity and AMS-^{14}C measurements in core 912A. Sediment cores 912A, 909B and 906B cover the last 600, 200 and 100 years respectively. Palynomorph influxes increase from the bottom to the top of each core, illustrating an increasing productivity over the last ~600 years until ~1850 AD, when we observe a decrease of productivity until today. We determined a succession of two assemblages over the last ~600 years. Assemblage I, at the base of each core, is mostly composed of dinocysts from heterotrophic taxa. The modern assemblage (Assemblage II at the top of each core) is mostly composed of dinocysts from autotrophic taxa. Quantitative reconstructions of sea-surface parameters reveal a sharp increase in summer (August) temperature (~2 to 5 °C) throughout the study area from ~1400 AD until ~1800–1850 AD, after which the increase (between ~0.5 and 1.0 °C) is much slower until modern times.

1. Introduction

Recent global climate change has focused Human's attention on the impact of anthropogenic activities on the planet. Scientists have begun looking at natural climate indicators as a means of measuring this impact, and reconstruct past climates to provide a basis for comparison. This research has revealed climatic cycles that are still poorly understood. The more we know about past climatic cycles, the more fully we can understand present conditions (Hansen et al., 2000; Watson et al., 2001; Alley et al., 2007).

The study of climatic variations in the Canadian Arctic, on time scales of 10 to 10,000 years, was one of the objectives of the CASES (Canadian Shelf Exchange Study) mission during the summer of 2004. Sea-surface conditions were reconstructed using dinoflagellate cyst assemblages, which are excellent indicators of sea-surface parameters (temperature, salinity, ice cover, primary productivity). The dinoflagellates are a group of microscopic unicellular biflagellate protists, some species of which can be toxic, forming what are known as red tides. The life cycle of some species comprises a dormancy phase during which the vegetative stages form cysts. The cyst's membrane is composed of a highly resistant polymer, dinosporin, allowing the cyst to be preserved in the sediment.

* Corresponding author.
E-mail address: thomas.richerol@uqar.qc.ca (T. Richerol).

The main objective of this article is to reconstruct past sea-surface temperature and salinity conditions and ice cover duration using dinocyst assemblages in three sedimentary sequences collected along a north–south transect in the Mackenzie Trough, located at the mouth of the Mackenzie River. Because the trough has the highest sedimentation rates in the study area, we were able to reconstruct approximately 100 to 600 years in the past. The chronology of our cores allows us to reconstruct climate changes during the post-industrial age (1850–2004 AD) and the Little Ice Age (LIA) (~1550–1850 AD). These three sedimentary sequences give us a more accurate picture of the period during which humans have had the most impact, and enable us to compare it with "natural" conditions in the past. We can thus better understand the current climate trend since the advent of significant human impact at the beginning of the Industrial Age, as well as the climatic changes associated with the Little Ice Age.

2. Environmental setting

The Mackenzie Shelf is a coastal region of the Beaufort Sea located along the Arctic Ocean's Canadian coast, between Point Barrow in northern Alaska and the western part of the Canadian Arctic Archipelago (C.A.A.) (Mudie and Rochon, 2001; Wang et al., 2005). It is approximately 100 km wide, representing less than 2% of the total coast of the Arctic Ocean, and covers an area of approximately 64,000 km² (to the 200 m isobath) (Stein and Macdonald, 2004; O'Brien et al., 2006). The shelf is bordered to the west by the Mackenzie Trough and to the east by Amundsen Gulf (Fig. 1). The ice cover varies greatly from year to year. In general, the ice begins to form in mid-October and begins to break up at the end of May (Wang et al., 2005; O'Brien et al., 2006). If the winds allow, the shelf may be ice-free as early as mid-July. In the winter, landfast ice forms near the coast, beyond the 20 m isobath, and the stamukhi (i.e. a field of ice fragments), which contains ice and sediment mixed together, form on the outer edge of the landfast ice. Beyond the stamukhi, one can observe a zone where the ice breaks up, with flaw lead forming intermittently across the pack ice, which tends to be moved westward by the Beaufort Gyre (Macdonald et al., 1995; O'Brien et al., 2006). To the east, near Amundsen Gulf, the ice-free zone forms part of the Cape Bathurst Polynya (Arrigo and van Dijken, 2004). Polynyas are ice-free zones in the middle of the landfast ice, in both the Arctic and the Antarctic, that form in the winter under the action of winds, currents and upwellings of warmer water. They form every year at approximately the same location and are, in general, areas of high productivity.

The Mackenzie is the third largest Arctic river in terms of flow of fresh water, with an average flow of 4000 m³/s (Melling, 2000; Dumas et al., 2005). It is also the largest in terms of sediment discharge, with approximately 127×10^6 Mt/year, which exceeds the total sediment discharge of all the other great Arctic rivers together (Macdonald et al., 2004; Stein and Macdonald, 2004; O'Brien et al., 2006). The Mackenzie River drainage basin, which is the source of the sediment and other materials carried by the river, covers a vast area (1.8×10^6 km²) (Hill et al., 2001; Wang et al., 2005; Abdul Aziz and Burn, 2006). This basin drains the northern Rockies Mountains through the Athabasca and Peace rivers, and the Mackenzie Mountains through the Nahanni, Liard and Peel rivers. The current system dates from the end of the Wisconsinian Glaciation and results from erosion by the Laurentide Ice Sheet, which shifted the eastward-flowing drainage system toward the north. The main part of the delta fills a glacial valley that runs the width of the Mackenzie Trough. This trough is composed of more than 200 m of glacial sediments from the end of the Pleistocene, covered with deltaic deposits from the end of the Pleistocene and the Holocene (Blasco et al., 1990; Hill, 1996; Hill et al., 2001).

The Mackenzie River flows into the Beaufort Sea. The oceanic circulation of the Beaufort Sea is dominated by the anticyclonic Beaufort Gyre, which pushes the currents along
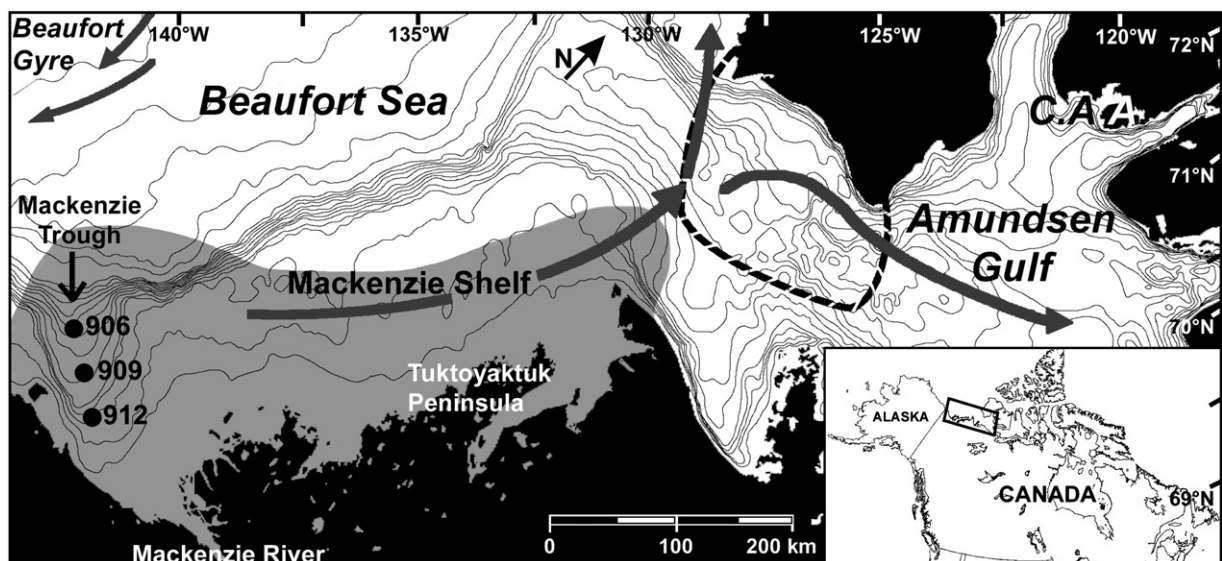
Fig. 1. Map of the Beaufort Sea, from the Mackenzie Trough to the Amundsen Gulf illustrating the sampling location of our three cores. The arrows represent the surface currents and the Beaufort Gyre, the zone in grey indicates the Mackenzie River plume influence and the dashed line indicates the Cap Bathurst Polynya.

the continental shelf. All along the coast, the currents are influenced by the wind direction, which alternates between eastward in the Canadian Archipelago and westward beyond the Mackenzie Trough (Vilks et al., 1979; Mudie and Rochon, 2001). The transport of suspended sediments within the plume of the Mackenzie river can be affected by the ice cover, winds and currents (Fig. 1). In winter, the river carries sediments on a shorter distance, and its flow rate is reduced near the coast, below the landfast ice (Macdonald et al., 1995). In summer, the plume's position is greatly affected by the winds. Those coming from the northeast push the plume along Tuktoyaktuk Peninsula (Giovando and Herlinveaux, 1981), while the winds from the southeast push the plume westward, beyond the Mackenzie Trough (MacNeill and Garrett, 1975). As a result, the highest rates of accumulation are found in the Mackenzie Trough and on the nearby continental slope. As we move farther to the east, the rates of accumulation decline up to Amundsen Gulf, where sediment hardly accumulates at all (Hill et al., 1991; Macdonald et al., 1998; Blasco, personnal communication).

The water column on the Mackenzie Shelf comprises three layers (Carmack et al., 1989): the surface layer (from 0 to ~30 m) is a mixed layer of polar water resulting from seasonal freshwater input and winter mixing. The intermediate layer has two strata of Pacific water, one of summer Pacific water (from ~50 to 80 m depth) warm, salty, oxygen-rich and nutrient-poor, and the other of winter Pacific water (at a depth of around ~150 m), colder, saltier, oxygen-poor and nutrient-rich. The bottom layer (at a depth of ~200 to 400 m), comprises cold, nutrient-poor water from the Atlantic with a salinity greater than 34. The intermediate and bottom layers have a cold halocline, the salinity increasing and the temperature decreasing with depth (Carmack et al., 1989; McLaughlin et al., 1996; McLaughlin et al., 2005; Lee and Whitledge, 2005).

During winter, and at the beginning of spring, the mix layer is rich enough in nutrients to support a phytoplanktonic bloom, but the ice cover inhibits light penetration. Phytoplankton (mainly ice algae) develops at the base of the ice layer, and at ice break-up almost all of it is carried to the bottom, supplying nutrients to benthic organisms. Light is thus a limiting factor during this season, while after spring break-up and during summer it is the nutrient supply that is limiting. At the end of winter, the halocline acts as a density barrier to nutrients, so that they remain outside the euphotic zone at the base of the mix layer (in the Pacific water layer) (Carmack et al., 2004). The initial nutrient supply is thus determined by the amount of river input. Moreover, the Mackenzie Trough is also subject to upwelling, which brings up saltier, nutrient-rich Pacific water (Iseki et al., 1987; Carmack et al., 1989; Carmack et al., 2004).

3. Materials and methods

3.1. Sampling

Sampling in the Beaufort Sea was carried out in the summer of 2004 during leg 8 of the CASES (Canadian Arctic Shelf Exchange Study) mission. Three sedimentary sequences were collected using PVC tubes inserted into box cores. Core 2004-804-912A (latitude 69°29.25N, longitude 137°56.43W, water depth 54 m, length 39 cm) was the closest to the shore, core 2004-804-909B (latitude 69°45.16N, longitude

138°16.296W, water depth 169 m, length 36 cm) in an intermediate position and core 2004-804-906B (latitude 70°01.145N, longitude 138°35.817W, water depth 272 m, length 34 cm) the farthest from the shore (Fig. 1). The three cores were described, and sampled at 1 cm intervals, at the Bedford Institute of Oceanography in Dartmouth, Nova Scotia. The palynological analyses were done at 2 cm intervals, while analysis for *Halodinium* sp. was carried out at 1 cm intervals in the upper 8 cm of core 906B. Each sample was then processed using the standard palynological method described by Rochon et al. (1999). For the reconstructions, we used dinoflagellate cysts as tracers of paleoceanographic conditions (sea-surface temperatures and salinities for summer and winter, and ice cover duration). Dinocysts are very useful, particularly in high latitude marine environments. The cyst's membrane is composed of a highly resistant polymer, dinosporin, which enables it to persist in sediments where siliceous (e.g. diatoms) and carbonate microfossils (e.g. coccoliths) are dissolved (de Vernal et al., 2001).

3.2. Sieving

From each sample, 5 cm^3 were collected by water displacement in a graduated cylinder and then transferred to a beaker. A tablet of *Lycopodium clavatum* spores of known concentration (12,100 spores) was added, acting as a palynological tracer that allows us to calculate each sample's palynomorph concentration. To determine the water content of the samples, a small quantity of sediment was collected and weighted before and after a minimum of 12 h in a drying oven (60 °C). The dried sediment was kept for subsequent ^{210}Pb chronology analyses. The rest of the sample was then put through 100 μm and 10 μm Nytex® sieves to eliminate a maximum of coarse sand, fine silts and clays. The 10–100 μm fraction was kept in a conical tube with a few drops of phenol for subsequent chemical processing.

3.3. Chemical processing

To dissolve the carbonates and silicates, the 10–100 μm fraction was treated with HCL (10%, 4 treatments) and HF (49%, 3 treatments, one at night), respectively. The acid treatments were carried out under a fume hood and were heated to increase the chemical reaction. The remaining fraction was rinsed with distilled water to eliminate all traces of acid before a final sieving at 10 μm to remove the fluorosilicates and fine particles. The sample was mixed in a Vortimixer, and a few drops of supernatant were mounted between a slide and cover slide in glycerine gel using a hot plate.

3.4. Palynomorph counts

Palynomorphs (pollen, spores, dinoflagellate cysts, acritarchs, freshwater algal cysts) were counted using transmitted light microscopy (Nikon Eclipse I-80) at 200× to 400×.

To obtain a good statistical representation of all taxa, a minimum of 300 dinoflagellate cysts were counted in most samples. However, in some samples (particularly core 2004-804-912A), the number of dinocysts was so low that we stopped counting as soon as we obtained a significant number of marker grains (in general more than 300 *Lycopodium* spores for less than 100 dinocysts) (Table 1). From these counts, we were able

Table 1
Dinocyst counts for each core

Depth (cm)	Total cysts	Marker grains	Ipal	Ocen	Pdal	Selo	Imin	Pame	Bspp	Squa	Parc
Core 2004-804-912A											
0	304	1675	0	137	65	11	60	0	28	0	3
2	311	1255	0	153	45	8	65	1	36	0	3
4	303	965	0	222	24	12	19	0	26	0	0
6	304	1017	0	139	80	3	49	0	29	1	3
8	309	1108	1	74	94	6	71	2	55	1	5
10	314	754	0	41	182	6	51	3	28	0	3
12	312	1041	1	54	147	4	58	5	40	0	3
14	148	1566	0	33	58	4	40	2	11	0	0
16	66	645	0	14	10	2	23	1	14	0	2
18	80	1124	0	19	4	0	32	0	23	0	2
20	59	1347	0	21	0	2	15	1	19	0	1
22	10	332	0	6	0	0	2	0	2	0	0
24	26	793	0	2	0	1	11	0	12	0	0
26	34	812	0	13	0	0	10	0	11	0	0
28	40	1200	0	8	0	0	5	0	27	0	0
30	91	2419	0	19	5	1	29	0	35	0	2
32	99	1337	0	1	51	0	17	0	29	0	1
34	140	1806	0	10	44	0	59	2	22	0	3
36	61	1664	0	0	19	0	34	0	8	0	0
38	168	3420	0	3	19	2	67	1	72	0	4
Core 2004-804-909B											
0	304	669	0	149	71	12	38	0	32	1	1
2	312	267	1	169	81	13	31	1	15	0	1
4	319	266	1	138	94	13	51	0	21	0	1
6	359	329	0	70	183	10	62	6	27	0	1
8	322	363	0	133	92	10	55	1	26	0	5
10	324	343	1	134	87	8	60	3	30	0	1
12	327	557	0	143	77	8	70	4	22	0	3
14	314	330	0	71	109	7	98	3	25	0	1
16	303	643	0	43	68	3	126	1	58	0	4
18	30	383	0	4	7	0	19	0	0	0	0
20	312	883	0	30	105	6	109	0	60	0	2
22	311	574	0	27	121	1	132	1	28	0	1
24	311	695	0	5	182	0	88	1	35	0	0
26	311	657	0	8	153	0	105	4	39	0	2
28	215	1554	0	8	56	0	84	1	61	0	5
30	313	876	1	6	48	0	204	3	50	0	1
32	305	1578	0	12	89	2	115	4	77	0	6
34	295	1644	3	34	49	7	110	8	77	0	7
36	309	1997	0	23	63	7	115	7	84	2	8
Core 2004-804-906B											
0	302	584	0	143	104	6	34	0	15	0	0
2	320	341	0	103	139	14	42	0	22	0	0
4	300	354	0	78	167	5	33	0	17	0	0
6	353	346	0	64	200	3	70	0	14	0	2
8	361	393	1	22	240	5	65	1	26	0	1
10	423	376	0	24	263	3	106	2	23	0	2
12	314	445	0	31	160	2	94	1	25	0	1
14	287	548	2	32	127	6	84	0	32	0	4
16	300	950	0	38	112	4	117	0	28	0	1
18	303	342	0	33	127	3	118	2	20	0	0
20	316	545	0	29	122	2	129	0	29	0	5
22	313	500	0	26	147	2	102	1	34	0	1
24	300	355	0	31	141	2	98	0	23	0	5
26	300	368	1	40	117	3	77	0	60	0	2
28	338	380	0	24	125	1	93	1	93	0	1
30	408	510	0	34	141	4	181	1	47	0	0
32	310	406	1	22	138	0	113	1	34	0	1
34	300	530	0	24	113	0	114	0	48	0	1

Ipal = *Impagidinium pallidum*; Ocen = *Operculodinium centrocarpum* + *Operculodinium centrocarpum* short spines; Pdal = *Pentapharsodinium dalei;* Selo = *Spiniferites elongatus* + *Spiniferites frigidus;* Imin = *Islandinium minutum* + *Islandinium minutum* var. *cezare;* Pame = *Protoperidinium americanum;* Bspp = *Brigantedinium* spp.; Squa = *Selenopemphix quanta;* Parc = *Polykrikos* var. arctic + *Polykrikos* var. quadratus + *Polykrikos schwartzii.*

to determine the concentration of dinoflagellate cysts per unit volume (cysts/cm^3) or per unit dry weight (cysts/g) and the relative abundance of each species (% dinocysts sp.) for each sample. The influxes of palynomorphs (grains/cm^2/year) can be calculated only for the depth where we have a sedimentation rate. However, the pattern of the curves of concentration and influx are similar for cores 912A and 909B and the trend are more accurate with the influx for the core 906B. The nomenclature used for identifying the dinocysts follows Rochon et al. (1999), Head et al. (2001) and the Lentin and Williams' index (Fensome and Williams, 2004).

Studies from Zonneveld et al. (1997, 2001) and Zonneveld and Brummer (2000) have shown species sensitivity to oxygen availability. The cysts from the *Protoperidinium* group are the most sensitive, followed by the genus *Spiniferites*, *Impagidinium* sp. and *Operculodinium centrocarpum*. The high sediment rates measured in the Mackenzie Trough helped preserve our dinocyst assemblages from oxidation, and the most sensitive taxa, such as *Brigantedinium* spp., show excellent preservation, with the operculum still attached on many specimens.

3.5. Chronological framework

Determination of an AMS-^{14}C age was performed on a shell found at 39 cm depth in the sediment core 912A. We determined an AMS-^{14}C age of 1420±40 AD (Lab-number BETA237046).

For the measurement of ^{210}Pb activity, the analyses were performed on the upper 20 cm of core 2004-804-912A and on the upper 15 cm of cores 2004-804-909B and 2004-804-906B. The rate of radioactive decay of ^{210}Pb allowed us to identify the age of our sediments. From radioactive decay curves we can determine an approximate natural supported ^{210}Pb activity value of 3 DPM (disintegrations per minute) for each core. From this value, we obtained the unsupported ^{210}Pb activity by deduction. Because we observed a constant exponential radioactive decay, we used the following formula from the CRS model (constant rate of ^{210}Pb supply from Appleby and Oldfield, 1983; Oldfield and Appleby, 1984);

$$t = -1/k \, * \, \mathrm{Ln} \, (A_0/A) \tag{1}$$

where t is the age of sediments at a given depth (year), k is the radioactive decay constant of ^{210}Pb (0.03114 year^{-1}; Roulet et al., 2000), A_0 is the unsupported activity of ^{210}Pb at the surface and A is the unsupported activity of ^{210}Pb at that depth.

If we assume that $\mathrm{Ln}(A_0/A)$ is the slope of the regression line of Ln (unsupported ^{210}Pb activity) as a function of depth, then:

$$\mathrm{Ln} \, (A_0/A) = -kt \tag{2}$$

and

$$t = \mathrm{Ln} \, (2)/22.3 \tag{3}$$

where 22.3 years is the half-life of ^{210}Pb. The sedimentation rate (Vs) is calculated thus;

$$Vs = - \, \mathrm{Ln} \, (2)/(slope*22.3). \tag{4}$$

The sedimentation rate enables us to calculate the age and date (t_0=2004 year) of the deepest sediments.

4. Results

4.1. Chronology

A bioturbation zone (Piot, 2007) was observed at the top of the cores collected closest to the mouth of the Mackenzie River, 4 cm from the surface of core 912A and 2 cm from the surface of core 909B (Fig. 2). The data from these zones were not used for establishing chronology by excess ^{210}Pb. Apart from these two bioturbation zones, the three cores display an exponential rate of radioactive decay with depth. In Ln (unsupported ^{210}Pb), we observe a change in the sedimentation rate for two cores: 909B and 906B (Fig. 2). We can thus calculate:

- For sequence 912A, the AMS-^{14}C age allows us to calculate a sedimentation rate of 0.494 cm/year between 40 and 20 cm, and the ^{210}Pb measurements indicate a sedimentation rate of 0.040 cm/year from 20 cm to the top of the core.
- For sequence 909B, a sedimentation rate of 0.084 cm/year was calculated from 15 cm to the top of the core, with a short episode with a lower sedimentation rate of 0.068 cm/year between 11.5 cm and 7.5 cm depth.
- For sequence 906B, a sedimentation rate of 0.226 cm/year from the depth of 15 cm of the core up to 11.5 cm, then 0.119 cm/year from 11.5 cm to the top of the core.

These sedimentation rates are in agreement with those previously published for our study area (Macdonald et al., 1998; O'Brien et al., 2006). We observe an increase of the sedimentation rate from the shore (912A) to the sea (906B), which illustrates the "bypass" phenomenon on the Mackenzie Shelf (Hill et al., 1991; Forest et al., 2008). Sediments and other fine particles are pushed out to sea by the current generated by the outflow of the river and are deposited in greater quantities on the slope than on the shelf.

We obtained a multi-decadal resolution for cores 912A and 909B, with samples recording approximately 20–30 years and 10–20 years, respectively, and a multi-annual resolution for core 906B, with samples representing approximately 5–10 years. Each core gives us a snapshot of a particular period: core 912A shows the last ~600 years with a focus on the LIA (~1550–1850 AD), and cores 909B and 906B show the Industrial Age period (~1850 to 2004 AD) (Fig. 2).

4.2. Stratigraphy of the three cores

The sediment composition of the three cores is relatively similar. The texture of the sediment is clayey and compact, and the water content decreases with depth. In the upper 5 cm, the sediment has a rusty colour indicating the oxic zone. Although there is little bioturbation, it is also in this zone that we find shell fragments and worm burrows. The rest of the core is greenish dark-grey to dark-grey; Munsel's index of 3/1 to 4/1.

Granulometric analyses show that the sediment column is divided into silts (62 μm to 4 μm) and clays (4 μm to 0.06 μm). The silts were mainly (~40 to 55%) fine (16 μm to 10 μm) to very fine (8 μm to 4 μm). Coarse silts (62 μm to 31 μm) and medium silts (31 μm to 20 μm) comprised less than ~25% of the silt fraction. Moving away from shore (from station 912A to station 906B), the proportion of fine to very fine silts decreased, while the clay portion increased.
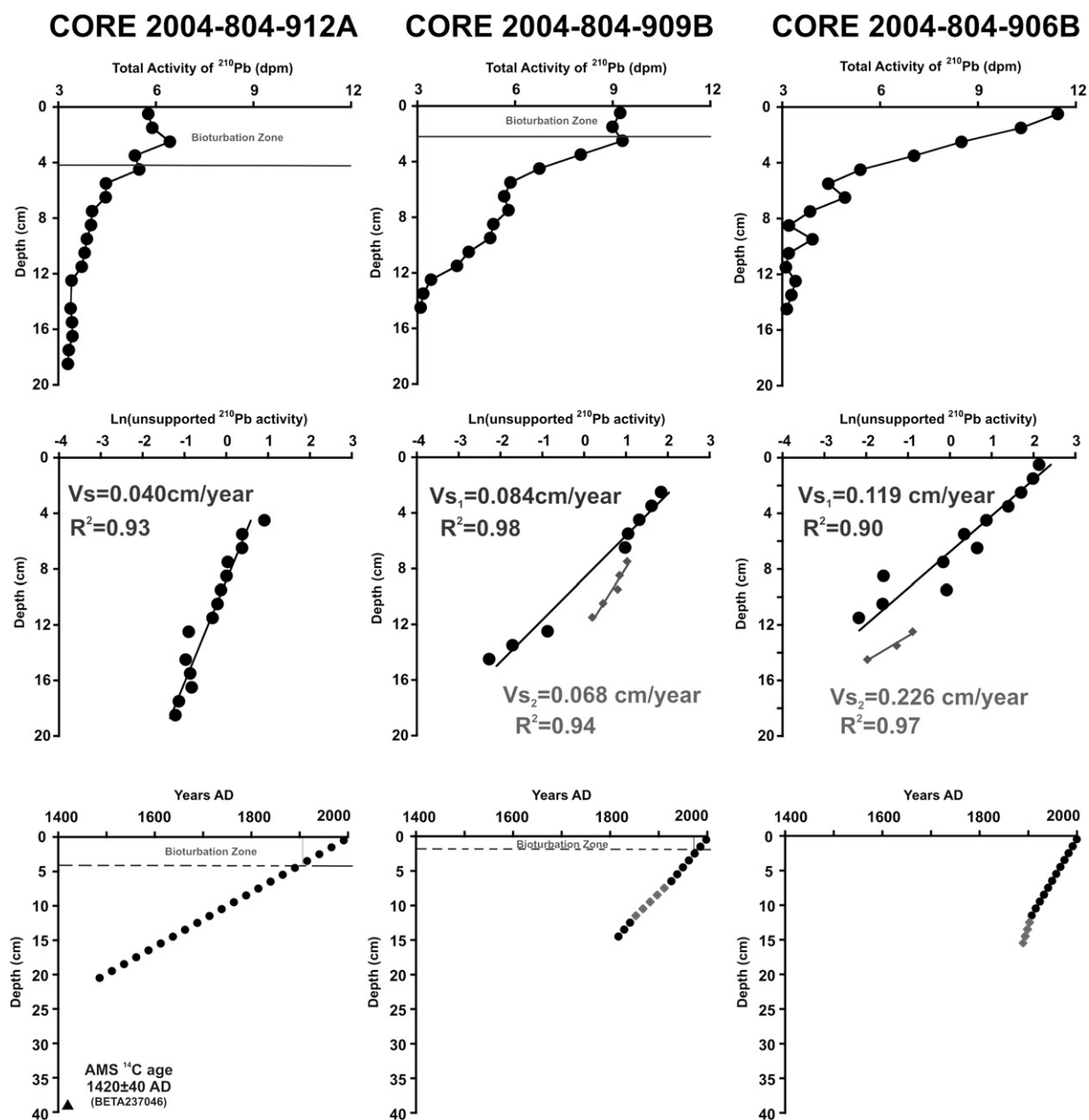
Fig. 2. Curves of the total activity of the ^{210}Pb (dpm), Ln (excess ^{210}Pb activity) and chronology (in years AD) according to depth in the sediments of the three cores. The second curve gives the sedimentation rate (cm/year). The triangle in the lower left corner indicates the AMS^{14}C age measured in core 912A.

Generally, the percentage of silts increased and that of clays decreased from the base to the top of the three sediment sequences. We observed an inverse relationship in core 912A, where the clays were more abundant than the silts in the first centimeter at the base.

4.3. Dinocyst assemblages

We used the free software ZONE created by Ph.D. Stephen Juggins (http://www.campus.ncl.ac.uk/staff/Stephen.Juggins/software.htm) to determine the dinoflagellate cyst assemblages in the three cores. We used the abundance (in percentage) of the six major species, without any transforma-

tion using the method of the Unweighted Least Squares Analysis (SPLITLSQ). We found two assemblages in each core (Fig. 3):

Assemblage I at the base of each core — characterised (~55% on average) by cysts of the heterotrophic dinoflagellates, *Islandinium minutum* s.l., *Brigantedinium* spp. and *Polykrikos* var. arctic/quadratus. We also counted cysts of the autotrophic dinoflagellate *Pentapharsodinium dalei*.

Assemblage II at the top of each core — the modern assemblage, characterised (~75% on average) by autotrophic species in the Beaufort Sea (Richerol et al., in press); *Operculodinium centrocarpum* s.l., *Pentapharsodinium dalei* and *Spiniferites elongatus/frigidus*.
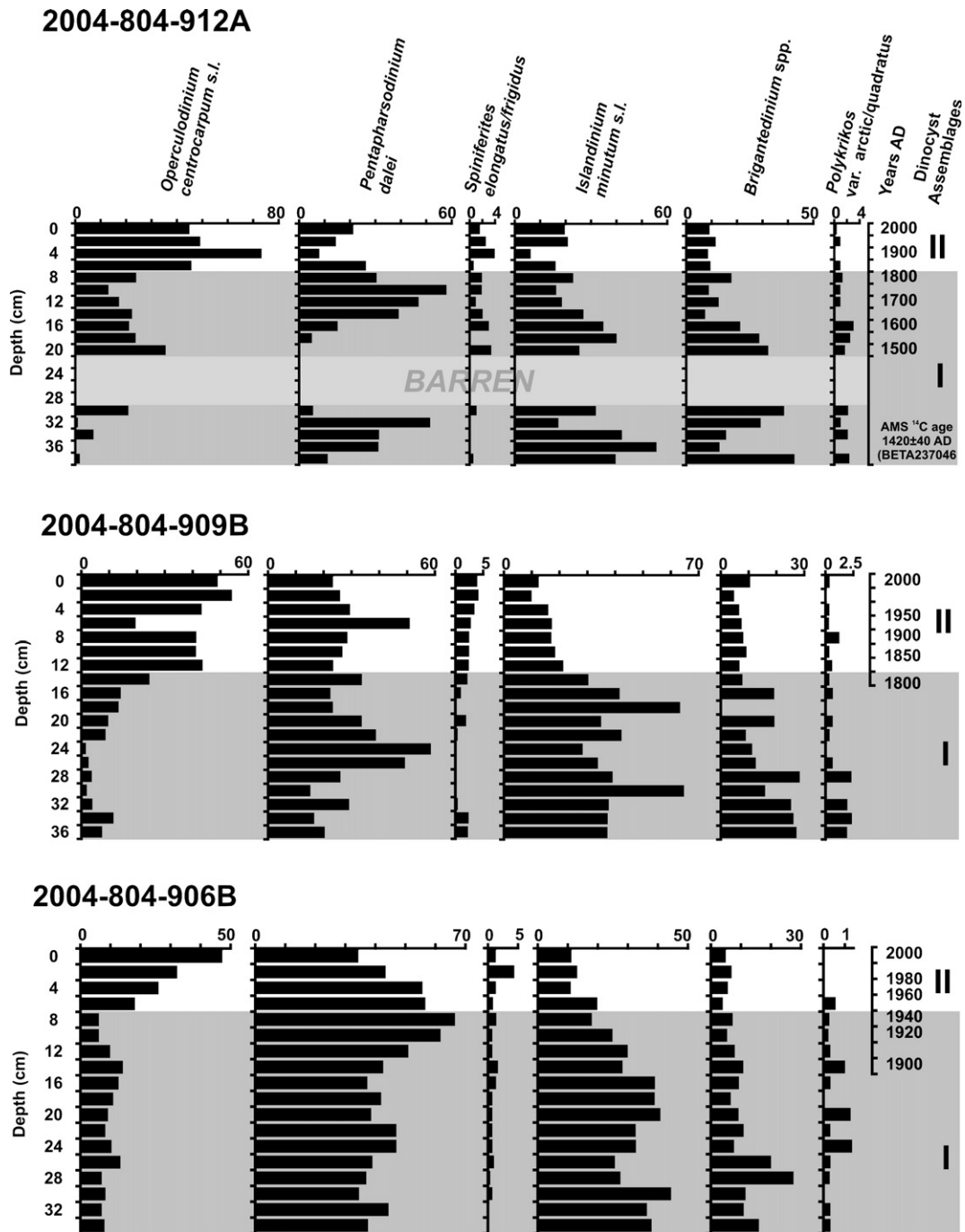
Fig. 3. Modern and fossil dinocyst assemblages identified from the relative abundance of major species for the three cores. The dark-grey zone represents Assemblage I. The light grey zone for core 912A represents the four sample depths considered "barren" after the count.

4.4. Palynomorph concentrations

We counted five types of palynomorphs (Fig. 4); dinocysts, *Halodinium* (an acritarch and freshwater tracer), terrestrial palynomorphs (pollen grains and spores, which allow us to compare terrestrial and marine climate changes), foraminifer linings, (indicators of benthic productivity; de Vernal et al., 1992; St-Onge et al., 1999), and reworked palynomorphs,

including dinocysts, pollen grains and spores (indicators of erosion).

In core 912A, we found a zone where the dinocyst assemblages were barren between 22 and 28 cm (~1438 to 1499 AD). Indeed, we counted very few dinocysts (10 to 40) for high numbers of marker grains (between 330 and 1200 *Lycopodium* spores). These four samples were not included in the paleoenvironmental reconstructions.

Core 2004-804-912A
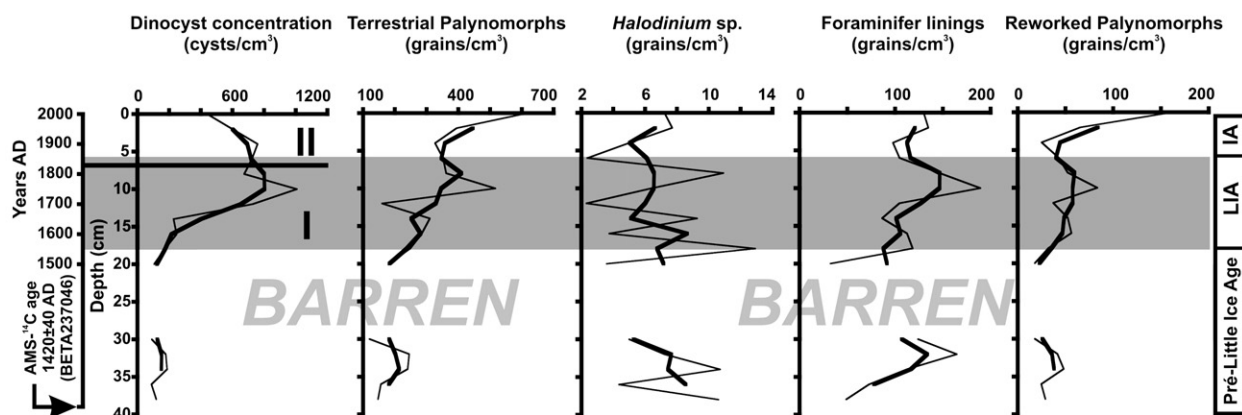
Core 2004-804-909B
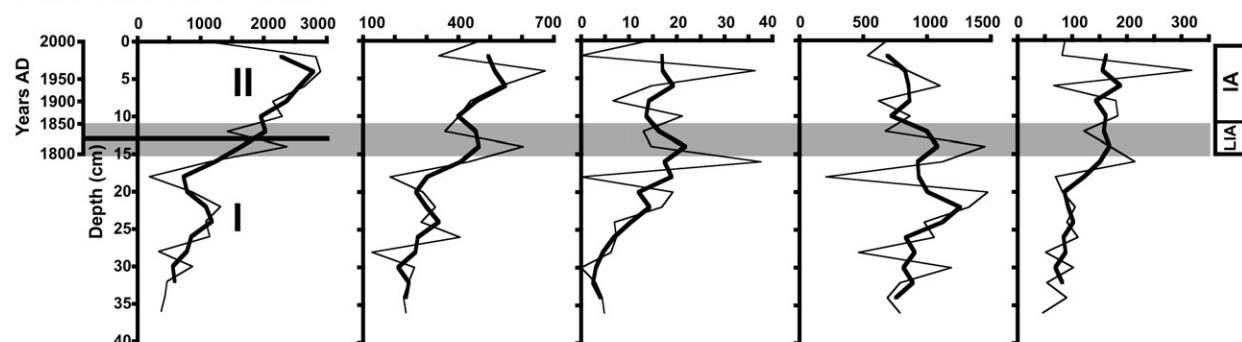
Core 2004-804-906B
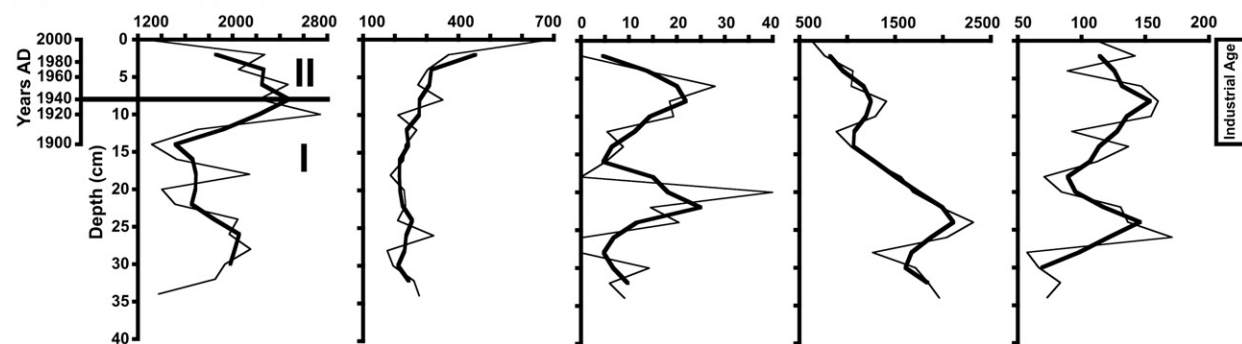
Fig. 4. Concentrations of the five types of palynomorphs counted, according to depth (cm), for each sediment core: dinocyst (cysts/cm³), terrestrial palynomorphs (grains/cm³), *Halodinium* (grains/cm³), foraminifer linings (linings/cm³) and reworked palynomorphs (grains/cm³). The "barren" zone for core 912A represents the four sample depths with low dinocyst count.

The freshwater palynomorph *Halodinium* sp. influxes can serve as an indicator of fluctuations in the Mackenzie River's flow (Fig. 5). Indeed, using river discharge data from Environment Canada's website (HYDAT software) covering the last ~70 years (~1935 to 2005 AD), we can see that during this period the fluctuations in *Halodinium* sp. influxes in sediment core 906B (farthest out to sea) coincide with variations in the Mackenzie river discharge. This suggests that the two are linked and that our data on *Halodinium* sp. fluctuations could serve as an indicator of freshwater input in

our study area. Because of the "bypass" phenomenon, *Halodinium* sp. influxes measured in sediment cores closer to the shore, and to the mouth of the river (912A and 909B), are weak and not very representative of the river discharge inflow or freshwater input.

4.5. Paleoceanographic reconstructions

The reconstruction of sea-surface parameters was performed with the software R (free software on the internet)
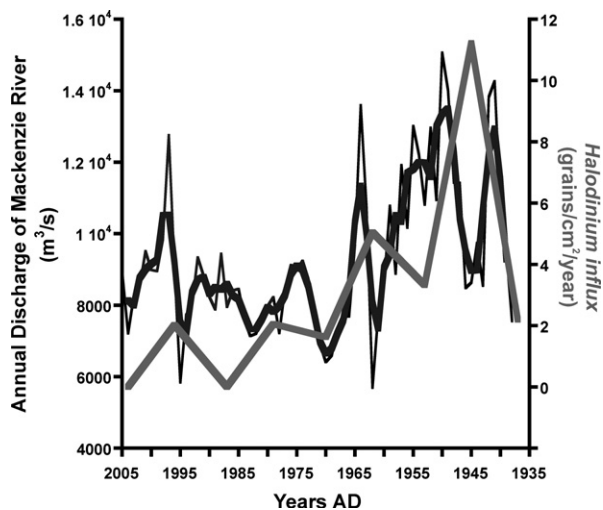
Fig. 5. Comparison between the annual inflow of the Mackenzie River (m³/s) from 1935 AD to 2005 AD, and the *Halodinium* influx (grains/cm²/year) for the same time-period, obtained from the core 906B. The data from the Mackenzie River discharge are from the HYDAT database on the Environment Canada website.

using transfer functions and the search for analogues in the GEOTOP database ($N=1171$). The descriptions of the results are organized in two parts for more convenience: the Little Ice Age (LIA) and the Industrial Age.

4.5.1. The LIA (~ 1550 to 1850 AD)

Data from core 912A give the general trend (resolution 1 sample every ~20–30 years) for our climate reconstructions during the LIA (1550–1850 AD). We observe a large increase in dinocyst influxes from the beginning of the LIA until ~1800 AD. The ratio of autotrophic to heterotrophic dinoflagellate cysts displays a shift from an assemblage dominated by heterotrophic dinoflagellates 600 years ago, to the modern assemblage dominated by autotrophic dinoflagellates (Richerol et al., in press). This shift is also illustrated by the transition, around 1825 AD, from assemblage I, dominated (55% on average) by heterotrophic dinoflagellate cysts, to assemblage II, dominated (75% on average) by autotrophic dinoflagellate cysts. At the beginning of the LIA, between ~1550 and ~1640 AD, summer temperature increases by ~2 °C, from ~3–4 °C to the current value of ~6 °C. The reconstructed temperature remains stable throughout the rest of the LIA. The salinity rapidly decreases at the beginning of the LIA (~1550 to 1650 AD), from ~27 to ~23 over ~100 years, and then remains constant until the end of the LIA. Ice cover duration is at a minimum (8 months/year) at the beginning of the LIA (~1550 AD) and increases by ~1.5 months/year during this period (Fig. 6).

4.5.2. The Industrial Age (~1850 to 2004 AD)

During the Industrial Age, the dinocyst influxes decrease, while the relative abundance of autotrophic dinoflagellate cysts continues to increase (between ~66% and ~85%), as recorded in core 912A (~1850 AD to the present). Summer temperature stabilises close to the modern value of 6 °C, salinity decreases from 23 to 20 and ice cover duration remains close to 9 months/year. Core 909B, in contrast to cores

912A and 906B, shows an increase in dinocyst influxes during the industrial period until ~1950 AD, followed by a decrease. The relative abundance of autotrophic dinoflagellate cysts also continues to rise (between ~70% and ~84%). Summer temperature rises slightly from ~5.5 to 6 °C, and salinity is close to its current value of 23. Ice cover duration remains between ~8.5 and 9 months/year.

Data from sequence 906B focus on the Industrial Age. From the end of the LIA, the dinocyst influxes begin to decrease, while the relative abundance of autotrophic dinoflagellate cysts continues to increase (between ~48% and ~83%). Summer temperature rises about 1 °C to its modern value of 6 °C. Salinity fluctuates between 23 and 25 in ~100 years. Reconstructions from 906B (the farthest from shore) are the only ones that show salinity values greater than 23 during the Industrial Age. The reconstruction of ice cover duration shows a small fluctuation between ~8 and 9 months/year (Fig. 6).

4.6. Validation test of the transfer functions

The dinocyst database ($n=1171$) was split in two parts (80/20) and a reconstruction was performed on the 20% part using the 80% part like a reference database. Instrumental values of temperature, salinity and sea-ice cover from the database were compared with the reconstructed values of the same parameters. The linearity of the relationship around a slope of one between estimates and observations provide a first indication of the reliability of the transfer functions. Moreover, we obtained a standard deviation value (RMSEP, Root Mean Square Error of Prediction) for each parameter that provides an estimation of the reliability of the reconstructions. We obtained an error of ±1.6 °C for the reconstructed August surface temperature, ±2.5 for the reconstructed August surface salinity, and ±1.1 months/year for the reconstructed sea-ice cover (Fig. 7).

On the whole, the validation test for the $n=1171$ database is similar to that obtained with the $n=677$ database (de Vernal et al., 2001). However, we observed an increase of the error for the reconstructed salinity compared to that of the previous version of the database ($n=371$; de Vernal et al., 1997; Rochon et al., 1999). This increase is explained by the important variability of this parameter. The increase of the prediction error for the salinity is also linked to the increase of the number of sites in the new database ($n=1171$). Therefore, reconstructions of low salinity values for the Arctic should always be interpreted with caution.

5. Discussion

The analysis of fossil dinocyst assemblages showed the existence of a "barren" zone in four samples from core 912A (22 to 28 cm). We did not include this zone in our reconstructions and interpretation because of the low cyst counts (e.g. 40 cysts per 1200 marker grains) and the absence of sedimentary evidence allowing us to identify a hiatus or abrupt sedimentary event (e.g. turbidite, slump). It could be that the dinocysts were not well preserved in the sediment (oxidation).

Dinocyst and terrestrial palynomorph (pollen grains and spores) concentrations fluctuate in a similar manner, possibly reflecting changes in sedimentation rate (Fig. 4). However, if we looked at the influxes where we had sedimentation rate,
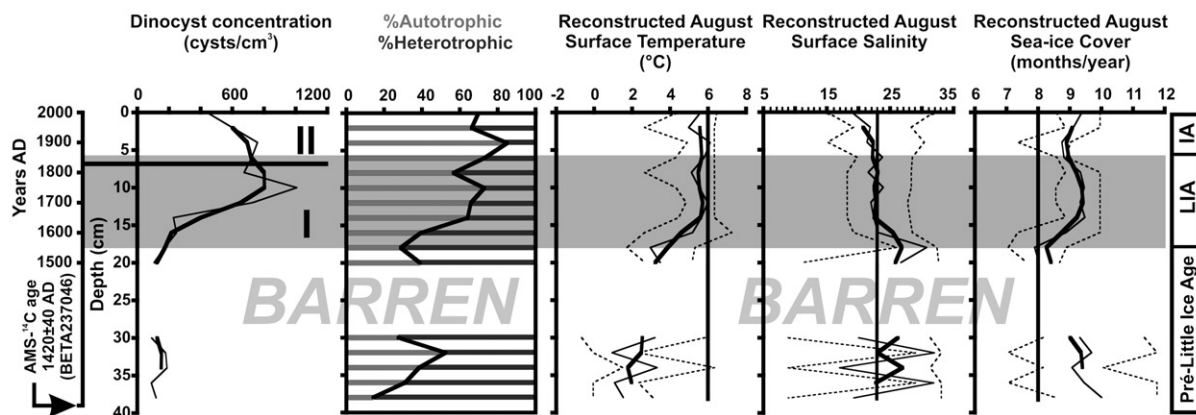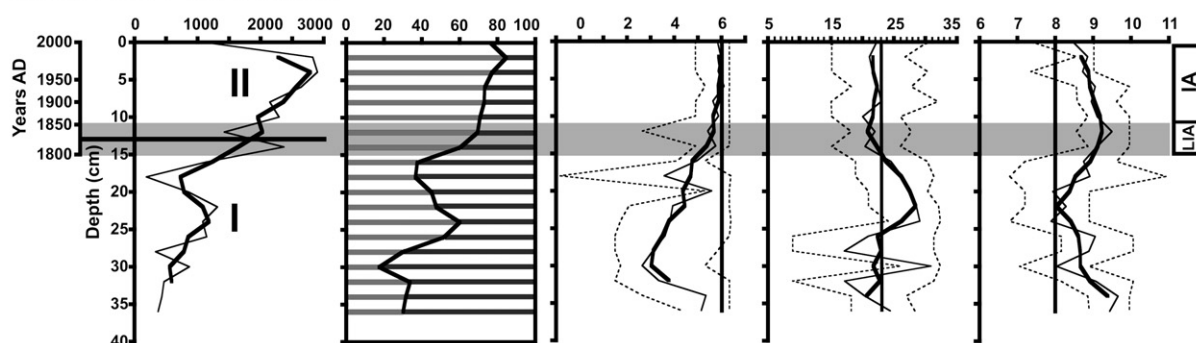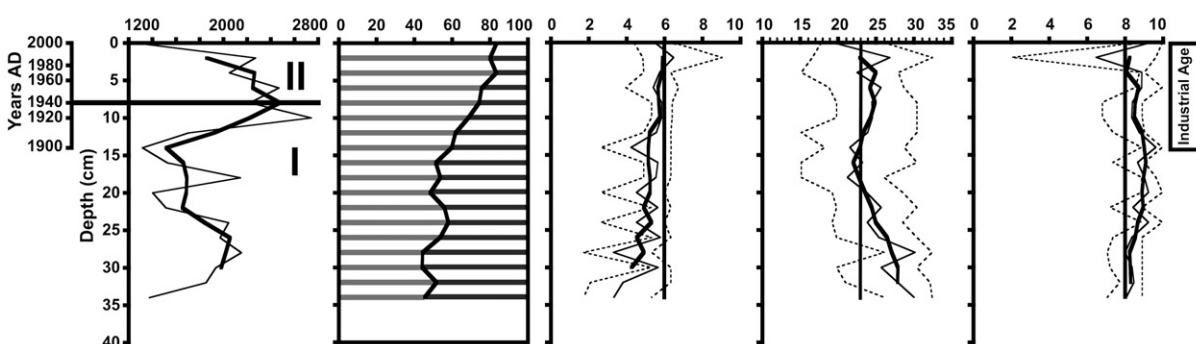
Fig. 6. Evolution of the dinocysts concentrations (cysts/cm³), the relative abundance of the cysts of autotrophic and heterotrophic dinoflagellates (%) and the three reconstructed oceanographic parameters: the August sea-surface temperature (°C), the August sea-surface salinity and the sea-ice cover duration (months/year). For each parameter, the vertical black line represents the modern value of the parameter. The "barren" zone for the core 912A represents the four sample depths with low dinocyst counts. The grey zone represents the Little Ice Age (~1550–1850 AD). The horizontal black line on the dinocysts influx curve represents the shift in dinocyst assemblage.

the parallel fluctuations observed in our sequences could be thus interpreted as synchronous variations in terrestrial and marine habitats.

Dinocyst and foraminifer lining influxes are good indicators of local pelagic and benthic productivity, respectively (de Vernal et al., 1992) (Fig. 4), and inform us about local carbon influxes to the sediment. The weak in-shore sedimentation causes most of the carbon to be carried out to sea and deposited on the slope.

Thus, these two palynomorphs' input to carbon influxes to the sediment increases outward from shore. However, it has decreased since ~1850 AD, the beginning of the Industrial Age, coinciding with a slightly declining sedimentation rate in core 906B and slower sedimentation in 909B between ~1800 and 1900 AD.

In general, our reconstructions based on dinocyst assemblages show an increase in sea-surface temperature from
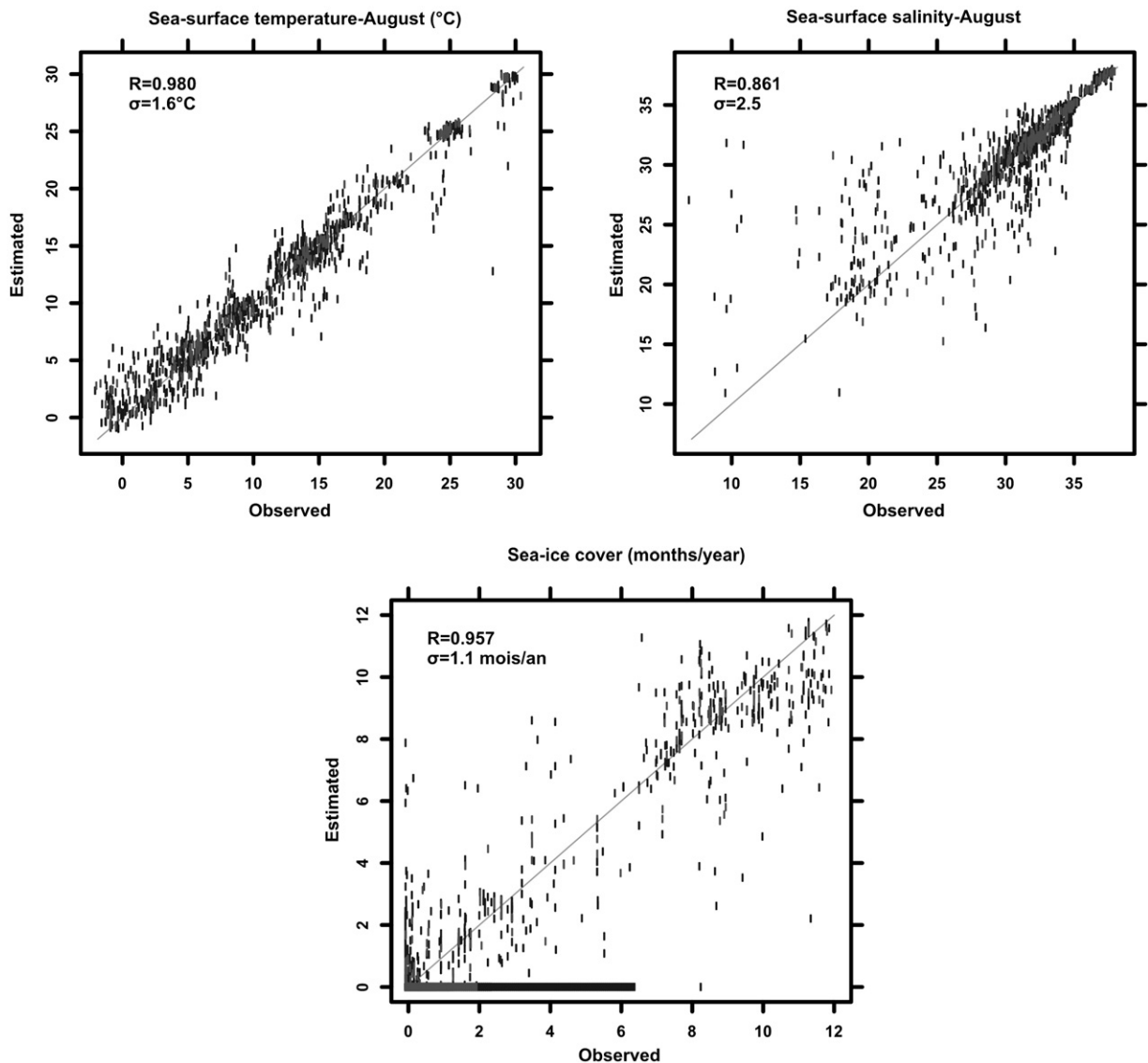
Fig. 7. Validation test of the transfer functions for the August sea-surface temperature (°C) and salinity, and the duration of the sea-ice cover (months/year). The grey dots represent the estimated values and the black dots the observed values.

~2 °C to 6 °C and a fluctuation in ice cover duration between ~8 and 10 months/year in the study area over the last 600 years (Fig. 6). Indeed, increased summer temperatures during the last millennium have been observed in high northern latitudes, interrupted by only one brief cold period during the LIA (~1550–1850) (Solomina and Alverson, 2004). The warming trend recorded in our cores was accompanied by a shift from heterotrophic to autotrophic-dominated dinoflagellate cyst assemblages (Fig. 3) in all three sequences (Fig. 6). However, the warming trend stabilised as of ~1850 AD, at the same time as the dinocyst influxes decreased (Fig. 6). This decrease is particularly evident in sequence 906B, although the proportion of autotrophic dinoflagellate cysts continues to rise. The recordings from the three sedimentary sequences, and their consecutive positions in the Mackenzie Trough, allow us to visualize a spatio-temporal shift asso-

ciated with the gradient from the fluvial influence of the Mackenzie River to the marine influence of the Beaufort Sea. The change in assemblage occurs later as we move out from shore (~1825 AD, ~1830 AD, ~1940 AD), and the transition from heterotrophic to autotrophic dominance of dinoflagellate cyst assemblages is also later farther from shore (Fig. 6). This shift occurs at the beginning of the LIA in 912A, the nearshore sequence, at the end of the LIA in 909B, in the intermediate position, and during the Industrial Age in 906B, farthest from shore. Moreover, the modern (~2004 AD) proportion of heterotrophic dinoflagellate cysts decreases seaward (~30%, ~20% and <20%). This concords with the distribution of modern dinocyst assemblages, which displays a gradient of heterotrophic to autotrophic-dominated dinocyst assemblages from the Mackenzie River plume's zone of influence out to sea and towards the Gulf of Amundsen

(Richerol et al., in press). There is also a clear time lag in the reconstructed parameters, suggesting earlier changes closer to shore and later ones out to sea.

Reconstructions from core 912A focus on the LIA (~1550–1850 AD: Fig. 6). It shows a cooling at the beginning of the LIA (~1550 AD), followed by an increase in summer temperature, which then slows down around 1630 AD. This slow-down comes later in the two others cores, ~1890 AD for the core 909B and ~1920 AD for the core 906B. Analysis of varved sediments from Lake Iceberg (Alaska) west of our study area and fed by melt water from three glaciers, permitted the reconstruction of temperature trends over a period of 1500 years (Loso et al., 2006). The varved sediments of Lake Iceberg record a decrease in temperature at the beginning of the LIA up until ~1650 AD, regarded as the LIA's minimum, followed by a warming trend that more or less flattens out around ~1800 and 1850 AD. Similarly, a cooling period at the beginning of the LIA in the 17th Century was recorded in ice cores from the Greenland ice cap (Fisher et al., 1998) and from temperature reconstructions based on changes in diatom communities in arctic and sub-arctic lakes (Rühland et al., 2003; Rühland and Smol, 2005; Smol et al., 2005; Michelutti et al., 2006). Our reconstructions for the Industrial Age (cores 909B and 906B; Fig. 6), suggest that the warming trend, while having slowed, has continued over the last ~150 years (~1 °C over 150 years). The behaviour of glaciers in the Canadian Arctic also suggests a warming trend. Although they expanded up until ~1850 AD, they have been retreating since that time (Miller et al., 2005). Glacier retreat, a worldwide phenomenon, coincides with the end of the LIA and the beginning of the Industrial Age (Dyurgerov and Meier, 2000). Changes in diatom communities, associated with a decrease in ice cover duration, have been observed since ~1850 AD in some lakes on Ellesmere Island (Michelutti et al., 2006) and in Slipper Lake, Northwest Territories, Canada (Rühland and Smol, 2005). A slight increase in pH (~0.3) in these lakes over the last ~150 years is also associated with the current warming trend. The increase in sea-surface temperature during the summer corresponds to an increase in summer air temperature. A similar rise, in the order of ~1.5 °C over ~100 years, was reconstructed from ~1900 AD to ~2004 AD for Alexandra Fjord on Ellesmere Island, Canada, based on growth patterns of the shrub *Cassiope tetragona* (Rayback and Henry, 2006). Our reconstructions also show a rise of ~1 °C in sea-surface temperature during the same period.

The stability of reconstructed summer temperature around its current value of 6 °C occurs later offshore due to the influence of colder water from the Beaufort Sea (~1630 AD, ~1890 AD, ~1920 AD) (Fig. 6). We know that freshwater from the Mackenzie River is warmer than the water in the Beaufort Sea (Carmack and Macdonald, 2002). The reduction in *Halodinium* sp. influxes (core 909B, Fig. 4) at the end of the LIA and during the Industrial Age, suggests a corresponding reduction in freshwater input. This decrease can partly explain the spatio-temporal deceleration of the warming trend from the shore out to sea, and over time since ~1850 AD. The decrease in river influence in space and time is also reflected in reconstructed salinity values (Fig. 6), which reach the current value of ~23 later as we move from the shore out to sea. During the Industrial Age, the sequences that were closest to shore, and thus the river's influence, (cores 912A and 909B) have salinities slightly lower than 23, while the sequence farthest out (core 906B) shows a slight increase in salinity since ~1900 AD, consistent with the decrease in the Mackenzie River discharge recorded since ~1935 AD (Fig. 5). We reconstructed a decrease in salinity between ~15 and 20 cm depth from sequence 906B (Fig. 6), corresponding to a peak in *Halodinium* sp. influxes, suggesting an increase in river discharge and freshwater input at the same period (Fig. 4). Therefore, the *Halodinium* sp. influxes reinforce our temperature and salinity reconstructions, independently of the dinocysts.

The minimum ice cover duration of ~8 months/year occurs later as we move farther from the shore (Fig. 6). There is also a decrease in ice cover duration during the Industrial Age corresponding to an increase in marine influence (from station 912A to station 906B). Analysis of annual lamina and diatom concentrations in sediment cores from an arctic lake in Nunavut (Devon Island, Canada) suggests a longer ice-free period or higher summer temperatures during the last ~100 years (Gajewski et al., 1997). A change of strategy (from benthic to planktonic) on the part of diatom communities has been observed in lakes all around the Arctic, due to longer ice-free periods (Rühland et al., 2003). The scale of these changes is a function of the temperature increase in each region (Smol et al., 2005).

The gradient in time and space from the shore out to sea is similar for all the reconstructed parameters; there is an inflexion point in all the parameter curves at the beginning or middle of the LIA near the shore, towards the end of the LIA in the intermediate position, and at the beginning of the Industrial Age for the sequence farthest from shore. We associate this spatio-temporal shift with a gradual decrease in the influence of the Mackenzie River. The decline of the influence of the Mackenzie River is particularly evident in reconstructed summer temperatures, which increase rapidly at the beginning of the LIA (Fig. 6) and more slowly towards the middle and end of the LIA at stations 912A and 909B, respectively. This abrupt change in temperature increase occurred around 1630 AD close to shore (core 912A) and is associated with a decrease in the Mackenzie River discharge and thus a decrease in the input of relatively warm freshwater. The decline in fresh water input is also reflected in the reconstructed salinity profile by an abrupt halt in the decrease in salinity during the same period (Fig. 6).

An assemblage dominated by autotrophic dinoflagellates suggests warmer conditions and a decrease in ice cover duration, favouring light penetration for photosynthesis (Wang et al., 2005). However, we did not observe a significant decline in ice cover duration. Another explanation for the increase in the proportion of autotrophic dinocyst species could be the water column's optical properties in the study area. The high degree of turbidity generated by the sediment load in the Mackenzie River inhibits light penetration for autotrophic dinoflagellates, favouring the development of heterotrophic species. The decreasing turbidity gradient in space (nearshore–offshore) and in time (associated with reduced river inflow) could explain the seaward increase in autotrophic dinoflagellate cysts over the last 600 years (Fig. 6). With the decline in river discharge suggested by our results (Figs. 4 and 5), there would be a decrease in sediment load, favouring the development of autotrophic dinoflagellates and an increase in the proportion of their cysts.

The proportion of autotrophic cysts can also be explained by limiting factors in the local food chain. Heterotrophic dino-flagellates feed mainly on marine diatoms and other dino-flagellates (Jacobson and Anderson, 1986, 1992; Hansen et al., 1996; Lee and Whitledge, 2005). The main source of nutrients for these primary producers comes from the Mackenzie River (Hsiao et al., 1977; Macdonald et al., 1998). In fact, diatoms are mainly found in the river's plume, despite the turbidity of the water. Planktonic production on the Mackenzie Shelf is limited by light in winter and at the beginning of spring, but in summer by nutrients, which depend on the stratification of the water column in the Beaufort Sea.

In the recordings in sedimentary core 909B, we observed a salinity peak at ~28 between 15 and 25 cm coinciding with a decrease in ice cover duration (from ~10 to 8 months/year). The paleoclimate of the Canadian Arctic over the last 1000 years has been reconstructed using ice cores (Fisher et al., 1998), lake sediments and tree rings (Gajewzki and Atkinson, 2003). The 1700s were relatively warm (although less so than currently) (Hughen et al., 2000; Gajewzki and Atkinson, 2003), and drier according to a recent study on sediments of a Yukon lake (Anderson et al., 2007). A decrease in precipitation could explain the salinity peak, reconstructed between 15 and 25 cm in sequence 909B, coinciding with an abrupt decrease in ice cover duration.

Current global warming is attributed to the release of anthropogenic greenhouse gases (Hansen et al., 2000; Watson et al., 2001; Alley et al., 2007). However, our reconstructions show that a continuous increase in summer sea-surface temperatures started before the onset of the LIA, thus before the Industrial Age, which suggests a natural warming trend, at least during the last ~600 years. On the other hand, we observed a slowing of this synchronous warming together with a large decrease in dinocyst productivity at the beginning of the Industrial Age (Fig. 6). This decrease in productivity could indicate anthropogenic effects superimposed on the natural climate trend. Our data suggest a slight increase in surface temperature of about 0.5 to 1.0 °C over the last ~200 years in the Beaufort Sea (Fig. 6), which is comparable to the increase in Arctic air temperature over the last ~150 years (Watson et al., 2001). Our climate reconstructions for the study zone are probably the result of a combination of local and global effects. However, they do not allow us to determine the relative importance of anthropogenic versus natural causes of global warming.

6. Conclusion

Reconstructions based on three sedimentary sequences collected in the Mackenzie Trough allowed us to document the evolution of paleoenvironmental conditions in this zone over a period of 600 years. Summer sea-surface temperatures increased, coinciding with a shift from an assemblage dominated by heterotrophic dinocysts (55% on average) before the beginning of the Industrial Age (~1800–1850 AD), to one dominated by autotrophic dinocysts (75% on average). However, the warming trend slowed around 1800–1850 AD and dinocyst influxes associated with the zone's productivity decreased.

Dinocyst assemblages and our reconstructed parameters change over both time and space in our study zone. We observed a decrease in the Mackenzie River's effect from the in-shore position (core 912A) out to sea (core 906B). Thus the shift to autotrophic dominance of the dinoflagellate cysts, the slowing of the warming trend, the decrease in salinity, the minimum ice cover duration, all happen later as we move farther from shore. The fact that a continuous increase in summer surface temperature began before the onset of the LIA, and thus well before the beginning of the Industrial Age, could suggest a natural warming trend rather than a man-made one. However, it is possible that the decrease in dinocyst productivity measured during the Industrial Age could be the result of anthropogenic activities.

References

Abdul Aziz, O.I., Burn, D.H., 2006. Trends and variability in the hydrological regime of the Mackenzie River Basin. Journal of Hydrology 319, 282–294.

Alley, R., Berntsen, T., Bindoff, N.L., Chen, Z., Chidthaisong, A., Friedlingstein, P., Gregory, J., Hegerl, G., Heimann, M., Hewitson, B., Hoskins, B., Joos, F., Jouzel, J., Kattsov, V., Lohmann, U., Manning, M., Matsuno, T., Molina, M., Nicholls, N., Overpeck, J., Qin, D., Raga, G., Ramaswamy, V., Ren, J., Rusticucci, M., Solomon, S., Somerville, R., Stocker, T.F., Stott, P., Stouffer, R.J., Whetton, P., Wood, R.A., Wratt, D., 2007. Climate change 2007; the physical science basis. Intergovernmental Panel on Climate Change (IPCC) 2007.

Anderson, L., Abbott, M.B., Finney, B.P., Burns, S.J., 2007. Late Holocene moisture balance variability in the southwest Yukon Territory, Canada. Quaternary Science Reviews 26, 130–141.

Appleby, P.G., Oldfield, F., 1983. The assessment of ^{210}Pb data from sites with varying sediment accumulation rates. Hydrobiologia 103, 29–35.

Arrigo, K.R., van Dijken, G.L., 2004. Annual cycles of sea ice and phytoplankton in Cape Bathurst Polynya, southeastern Beaufort Sea, Canadian Arctic. Geophysical Research Letters 31, L08304.

Blasco, S.M., Fortin, G., Hill, P.R., O'Connor, M.J., Brigham-Grette, J.K., 1990. The Late Neogene and Quaternary stratigraphy of the Canadian Beaufort continental shelf. In: Grantz, A., Johnson, L., Sweeney, J.F. (Eds.), The Arctic Ocean region. Geological Society of America, The Geology of North America, Vol. L, pp. 491–502.

Carmack, E.C., Macdonald, R.W., 2002. Oceanography of the Canadian Shelf of the Beaufort Sea; a setting for marine life. Arctic 55 (1), 29–45.

Carmack, E.C., Macdonald, R.W., Papadakis, J.E., 1989. Water mass structure and boundaries in the Mackenzie Shelf estuary. Journal of Geophysical Research 94 (C12), 18043–18055.

Carmack, E.C., Macdonald, R.W., Jasper, S., 2004. Phytoplankton productivity on the Canadian Shelf of the Beaufort Sea. Marine Ecology Progress Series 277, 37–50.

de Vernal, A., Bilodeau, G., Hillaire-Marcel, C., Kassou, N., 1992. Quantitative assessment of carbonate dissolution in marine sediments from foraminifer

linings vs. shell ratios; Davis Strait, Northwest North Atlantic. Geology 20 (6), 527–530.

de Vernal, A., Rochon, A., Turon, J.-L, Matthiessen, J., 1997. Organic-walled dinoflagellate cysts: palynological tracers of sea-surface conditions in middle to high latitude marine environments. GEOBIOS 30 (7), 905–920.

de Vernal, A., Henry, M., Matthiessen, J., Mudie, P.J., Rochon, A., Boessenkool, K.P., Eynaud, F., Grøsfjeld, K., Guiot, J., Hamel, D., Harland, R., Head, M.J., Kunz-Pirrung, M., Levac, E., Loucheur, V., Peyron, O., Pospelova, V., Radi, T., Turon, J.-L., Voronina, E., 2001. Dinoflagellate cyst assemblages as tracers of sea-surface conditions in the northern North Atlantic, Arctic and sub-Arctic seas; the new '*n*=677' data base and its application for quantitative palaeoceanographic reconstruction. Journal of Quaternary Science 16 (7), 681–698.

Dumas, J., Carmack, E., Melling, H., 2005. Climate change impacts on the Beaufort shelf landfast ice. Cold Regions Science and Technology 42, 41–51.

Dyurgerov, M.B., Meier, M.F., 2000. Twentieth century climate change; evidence from small glaciers. Presentation of the National Academy of Sciences of the USA 97 (4), 1406–1411.

Fensome, R.A., Williams, G.L., 2004. The Lentin and Williams Index of Fossil Dinoflagellates. Contribution Series Number 42. American Association of Stratigraphic Palynologists Foundation, Dallas, TX.

Fisher, H., Werner, M., Wagenbach, D., Schwager, M., Thorsteinnson, T., Wilhelms, F., Kipfstuhl, J., Sommer, S., 1998. Little Ice Age clearly recorded in northern Greenland ice cores. Geophysical Research Letters 25 (10), 1749–1752.

Forest, A., Sampei, M., Hattori, H., Makabe, R., Sasaki, H., Fukuchi, M., Wassmann, P., Fortier, L., 2008. Particulate organic carbon fluxes on the slope of the Mackenzie Shelf (Beaufort Sea): physical and biological forcing of shelf-basin exchanges. Journal of Marine Systems 68, 39–54.

Gajewzki, K., Atkinson, D.A., 2003. Climatic change in northern Canada. Environmental Reviews 11, 69–102.

Gajewski, K., Hamilton, P.B., McNeely, R., 1997. A high resolution proxy-climate record from an arctic lake with annually-laminated sediments on Devon Island, Nunavut, Canada. Journal of Paleolimnology 17 (2), 215–225.

Giovando, L.F., Herlinveaux, R.H., 1981. A discussion of factors influencing dispersion of pollutants in the Beaufort Sea. Pacific Marine Science Report 81 (4), 198.

Hansen, B., Christiansen, S., Pedersen, G., 1996. Plankton dynamics in the marginal ice zone of the central Barents Sea during spring; carbon flow and structure of the gazer food chain. Polar Biology 16, 115–128.

Hansen, J., Sato, M., Ruedy, R., Lacis, A., Oinas, V., 2000. Global warming in the twenty-first century: an alternative scenario. Proceedings of the National Academy of Sciences of the United States of America 97 (18), 9875–9880.

Head, M.J., Harland, R., Matthiessen, J., 2001. Cold marine indicators of the late Quaternary; the new dinoflagellate cyst genus Islandinium and related morphotypes. Journal of Quaternary Science 16 (7), 621–636.

Hill, P.R., 1996. Late Quaternary sequence stratigraphy of the Mackenzie Delta. Canadian Journal of Earth Science 33, 1064–1074.

Hill, P.R., Blasco, S.M., Harper, J.R., Fissel, D.B., 1991. Sedimentation on the Canadian Beaufort Shelf. Continental Shelf Research 11 (8–10), 821–842.

Hill, P.R., Lewis, C.P., Desmarais, S., Kauppaymuthoo, V., Rais, H., 2001. The Mackenzie Delta: sedimentary processes and facies of a high-latitude, fine-grained delta. Sedimentology 48, 1047–1078.

Hsiao, S.I.C., Foy, M.G., Kittle, D.W., 1977. Standing stock, community structure, species composition, distribution, and primary production of natural populations of phytoplankton in the southern Beaufort Sea. Canadian Journal of Botany 55, 685–694.

Hughen, K.A., Overpeck, J.T., Anderson, R.F., 2000. Recent warming in a 500-year palaeotemperature record from varved sediments, Upper Soper Lake, Baffin Island, Canada. The Holocene 10 (1), 9–19.

Iseki, K., Macdonald, R.W., Carmack, E., 1987. Distribution of particulate matter in the southeastern Beaufort Sea in late summer. Polar Biology 1, 35–46.

Jacobson, D.M., Anderson, D.M., 1986. Thecate heterotrophic dinoflagellates: feeding behavior and mechanisms. Journal of Phycology 22, 249–258.

Jacobson, D.M., Anderson, D.M., 1992. Ultrastructure of the feeding apparatus and myonemal system of the heterotrophic dinoflagellate *Protoperidinium spinulosum*. Journal of Phycology 28 (1), 69–82.

Lee, S.H., Whitledge, T.E., 2005. Primary and new production in the deep Canada Basin during summer 2002. Polar Biology 28, 190–197.

Loso, M.G., Anderson, R.S., Anderson, S.P., Reimer, P.J., 2006. A 1500-year record of temperature and glacial response inferred from varved Iceberg Lake, southcentral Alaska. Quaternary Research 66 (1), 12–24.

Macdonald, R.W., Paton, D.W., Carmack, E.C., Omstedt, A., 1995. The freshwater budget and under-ice spreading of Mackenzie River water in the Canadian Beaufort Sea based on salinity and $^{18}O/^{16}O$ measurements in water and ice. Journal of Geophysical Research 100, 895–919.

Macdonald, R.W., Solomon, S.M., Cranston, R.E., Welch, H.E., Yunker, M.B., Gobeil, C., 1998. A sediment and organic carbon budget for the Canadian Beaufort Shelf. Marine Geology 144, 255–273.

Macdonald, R.W., Naidu, A.S., Yunker, M.B., Gobeil, C., 2004. The Beaufort Sea: distribution, sources, fluxes and burial of organic carbon. In: Stein, R., Macdonald, R.W. (Eds.), The Organic Carbon Cycle in the Arctic Ocean. Springer Publishing Company, Berlin, pp. 177–193.

McLaughlin, F.A., Carmack, E.C., Macdonald, R.W., Bishop, J.K.B., 1996. Physical and geochemical properties across the Atlantic/Pacific water mass front in the southern Canada Basin. Journal of Geophysical Research 101 (C1), 1183–1197.

McLaughlin, F., Shimada, K., Carmack, E., Itoh, M., Nishino, S., 2005. The hydrography of the southern Canada Basin, 2002. Polar Biology 28, 182–189.

MacNeill, M.R., Garrett, J.F., 1975. Open water surface currents. Beaufort Sea Technical Report 17, 113.

Melling, H., 2000. Exchanges of freshwater through the shallow straits of the North American Arctic. In: Lewis, E.L., Jones, E.P., Lemke, P., Prowse, T.D., Wadhams, P. (Eds.), The Freshwater Budget of the Arctic Ocean. NATO Science Partnership Sub-series; 2, Environmental Security Volume 70. Kluwer Academic Publishers, Dordrecht, pp. 479–502.

Michelutti, N., Douglas, M.S.V., Wolfe, A.P., Smol, J.P., 2006. Heightened sensitivity of a poorly buffered high arctic lake to late-Holocene climatic change. Quaternary Research 65, 421–430.

Miller, G.H., Wolfe, A.P., Briner, J.P., Sauer, P.E., Nesje, A., 2005. Holocene glaciation and climate evolution of Baffin Island, Arctic Canada. Quaternary Science Reviews 24, 1703–1721.

Mudie, P.J., Rochon, A., 2001. Distribution of dinoflagellate cysts in the Canadian Arctic marine region. Journal of Quaternary Science 16 (7), 603–620.

O'Brien, M.C., Macdonald, R.W., Melling, H., Iseki, K., 2006. Particle fluxes and geochemistry on the Canadian Beaufort Shelf: implications for sediment transport and deposition. Continental Shelf Research 26, 41–81.

Oldfield, F., Appleby, P.G., 1984. Empirical testing of ^{210}Pb-dating models for lake sediment. In: Haworth, E.Y., Lund, J.W.G. (Eds.), Lake Sediments and Environmental History. University of Minnesota Press, p. 93.

Piot, A., 2007. Étude expérimentale de l'influence de la bioturbation exercée par les annélides Nephtys caeca (Fabricius) et Nereis virens (Sars) sur la répartition des kystes de dinoflagellés dans le sédiment. Mémoire de Maîtrise en Océanographie déposé à l'Université du Québec à Rimouski.

Rayback, S.A., Henry, G.H.R., 2006. Reconstruction of summer temperature for a Canadian high arctic site from retrospective analysis of the dwarf shrub, *Cassiope tetragona*. Arctic, Antarctic, and Alpine Research 38 (2), 228–238.

Richerol, T., Rochon, A., Blasco, S., Scott, D., Schell, T., Bennett, R., in press. Distribution of dinoflagellate cysts in surface sediments of the Mackenzie Shelf and Amundsen Gulf, Beaufort Sea (Canada). Journal of Marine Systems. doi:10.1016/j.jmarsys.2007.11.003.

Rochon, A., de Vernal, A., Turon, J.-L., Matthiessen, J., Head, M.J., 1999. Distribution of Recent Dinoflagellate Cysts in Surface Sediments from the North Atlantic Ocean and Adjacent Seas in Relation to Sea-surface Parameters. Contribution Series Number 35. American Association of Stratigraphic Palynologists Foundation, Dallas, TX. 152pp.

Roulet, M., Lucotte, M., Canuel, R., Farella, N., Courcelles, M., Guimarães, J.-R.D., Mergler, D., Amorim, M., 2000. Increase in mercury contamination recorded in lacustrine sediment following deforestation in the central Amazon. Chemical Geology 165, 243–266.

Rühland, K., Smol, J.P., 2005. Diatom shifts as evidence for recent Subartic warming in a remote tundra lake, NWT, Canada. Palaeogeography, Palaeoclimatology, Palaeoecology 226, 1–16.

Rühland, K., Priesnitz, A., Smol, J.P., 2003. Paleolimnological evidence from diatoms for recent environmental changes in 50 lakes across Canadian Arctic Treeline. Arctic, Antarctic, and Alpine Research 35 (1), 110–123.

Smol, J.P., Wolfe, A.P., Birks, H.J.B., Douglas, M.S.V., Jones, V.J., Korhola, A., Pienitz, R., Rühland, K., Sorvari, S., Antoniades, D., Brooks, S.J., Fallu, M.-A., Hughes, M., Keatley, B.E., Laing, T.E., Michelutti, N., Nazarova, L., Nyman, M., Paterson, A.M., Perren, B., Quinlan, R., Rautio, M., Saulnier-Talbot, E., Siitonen, S., Solovieva, N., Weckström, J., 2005. Climate-driven regime shifts in the biological communities of arctic lakes. Presentation of the National Academy of Sciences of the USA 102 (12), 4397–4402.

Solomina, O., Alverson, K., 2004. High latitude Eurasian paleoenvironments: introduction and synthesis. Palaeogeography, Palaeoclimatology, Palaeoecology 209, 1–18.

Stein, R., Macdonald, R.W., 2004. The Organic Carbon Cycle in the Arctic Ocean. Springer, Berlin. 363pp.

St-Onge, G., Leduc, J., Bilodeau, G., de Vernal, A., Devillers, R., Hillaire-Marcel, C., Loucheur, V., Marmen, S., Mucci, A., et Zhang, D., 1999. Caractérisation des sédiments récents du fjord du Saguenay (Québec) à partir de traceurs physiques, géochimiques, isotopiques et micropaléontologiques. Géographie Physique et Quaternaire 53 (3), 339–350.

Vilks, G., Wagner, F.J.E., Pelletier, B.R., 1979. The Holocene marine environment of the Beaufort Shelf. Geological Survey of Canada Bulletin 303 43pp.

Wang, J., Cota, G.F., Comiso, J.C., 2005. Phytoplankton in the Beaufort and Chukchi seas; distribution, dynamics, and environmental forcing. Deep-Sea Research II 52, 3355–3368.

Watson, R.T., Albritton, D.L., Barker, T., Bashmakov, I.A., Canziani, O., Christ, R., Cubasch, U., Davidson, O., Gitay, H., Griggs, D., Halsnaes, K., Houghton, J., House, J., Kundzewicz, Z., Lal, M., Leary, N., Magadza, C., McCarthy, J.J., Mitchell, J.F.B., Moreira, J.R., Munasinghe, M., Noble, I., Pachauri, R., Pittock, B., Prather, M., Richels, R.G., Robinson, J.B., Sathaye, J., Schneider, S., Scholes, R., Stocker, T., Sundararaman, N., Swart, R., Taniguchi, T., Zhou, D., 2001. Climate change 2001: synthesis report. Intergovernmental Panel on Climate Change (IPCC) 2001.

Zonneveld, K.A.F., Brummer, G.-J.A., 2000. (Palaeo-)ecological significance, transport and preservation of organic-walled dinoflagellate cysts in the Somali Basin, NW Arabian Sea. Deep-Sea Research II 47, 2229–2256.

Zonneveld, K.A.F., Versteegh, G.J.M., de Lange, G.J., 1997. Preservation of organic-walled dinoflagellate cysts in different oxygen regimes: a 10,000 years natural experiment. Marine Micropaleontology 29, 393–405.

Zonneveld, K.A.F., Versteegh, G.J.M., de Lange, G.J., 2001. Palaeoproductivity and post-depositional aerobic organic matter decay reflected by dino-flagellate cyst assemblages of the Eastern Mediterranean S1 sapropel. Marine Geology 172, 181–195.

Electronic references

Environment Canada Website — Archived Hydrometric Data (HYDAT) URL; http://www.wsc.ec.gc.ca/hydat/H2O/index_e.cfm?cname=main_e.cfm.

The R project for statistical computing URL; http://www.r-project.org.